

Curvilinear coordinates for full-core atoms

A. Putrino and G. B. Bachelet

*Istituto Nazionale di Fisica della Materia (INFM) and Dipartimento di Fisica
Università di Roma La Sapienza, Piazzale Aldo Moro 5, I-00185 Rome, Italy*

Abstract

Curvilinear coordinates, introduced by F. Gygi for valence-only solids and molecules within the local-density functional theory, can be used to describe both core and valence states in electronic-structure calculations. A simple and quite general coordinate transformation results in a large, yet affordable plane-wave energy cutoff for full-core systems (e.g., $\simeq 120$ Ryd for carbon or silicon) within the local-density functional theory, and in a reduced correlation time for full-core variational Monte Carlo calculations. Numerical tests for isolated Li, C, and Si atoms are presented.

1 Introduction

The study of electrons in atoms, molecules and solids represents a very active front of computational and theoretical physics, where the frontiers of quantum statistical mechanics and materials science blend. In the last 15 years at least two major innovations emerged in the context of large-scale electronic-structure calculations. One is the Car-Parrinello method [1], by which, within the Local Density Approximation (LDA) of the Density Functional Theory (DFT), the simultaneous time evolution of ionic positions and electronic wavefunctions became possible for realistic molecular or solid-state systems; in a sense, this is the most mature outcome of traditional self-consistent-field approaches. Another is the new family of quantum Monte Carlo (QMC) methods, which use random numbers to sample realistic many-electron wavefunctions; their stage of development is less mature (the ionic motion is still out of the question), but they have already explored the electronic states of a number of atoms, molecules and solids, and appear as a promising tool for the future [2].

Although their theoretical background and the corresponding computational strategies are quite different, both of these innovations have until now heavily relied on some pseudopotential approximation of the electron-ion interactions. Real electrons in a coulombic nuclear potential are arranged according to the shell structure typical of atoms, and, unless the physically relevant valence information is extracted by some approximate valence-only scheme, most of the computational effort of either DFT or QMC methods is wasted in the great multiplicity of length and energy scales of inner, or core shells. From this point of view the pseudopotential approximation [3] usually does an excellent job, as witnessed by its extensive application to molecular and solid-state problems, but full-core approaches [4], whenever possible, remain attractive, both for their ability to avoid ambiguities in those cases where the core-valence separation is less obvious, and, as we recall in a moment, for the less firm theoretical basis of pseudopotentials within the new Monte Carlo schemes.

In this paper we propose a new method, based on curvilinear coordinates (hereafter CC), by which the valence properties of full-core atoms, rather than pseudo atoms, can be efficiently described in connection with both density functionals and variational Monte Carlo schemes. In the remainder of this introduction we give a brief overview on the core-valence problem, which should highlight the background and motivations of our method, presented in Section 2. Section 3 will be devoted to numerical results on isolated atoms, and Section 4 will present some conclusions and perspectives.

1.1 *Full-core methods within the LDA*

For isolated atoms, in spite of the many different length scales induced by the electronic shell structure as the atomic number Z grows from 1 to 100, the use of radial logarithmic grids (with exponentially variable step, very dense near the nucleus, less and less dense towards the farther regions) allows an extremely accurate description of any atom in the Periodic Table of the Elements with just a few ($\simeq 200$) radial points, sometimes much less [5]. After the advent of energy-linearized schemes [4], this grid became a useful and effective tool also for solids or molecules, in connection either with atomic-sphere approximations (originally intended for closed-packed systems), or with a convenient partition of space (atomic spheres and interstitial regions). In this case, however, the basis functions are quite different from plane waves or energy-independent atomic orbitals: the application of linear muffin-tin orbitals (LMTO) to open systems, like tetrahedrally bonded semiconductors or surfaces, required considerable theoretical developments [6], and, at least up to now, even the powerful linear augmented plane waves (LAPW) [7] have not been used for Car-Parrinello-like molecular dynamics schemes.

1.2 *Pseudopotentials*

Smooth valence-only potentials which effectively replace the core electrons and the sharp nuclear coulomb singularity which binds them, or pseudopotentials, have always provided an attractive alternative. In the late seventies and early eighties they acquired, within the DFT, explicit relations to the full-core atom, and became “first-principles” pseudopotentials [3]. The price to pay for such a major upgrade was their angular nonlocality, which mainly reflects the different orthogonality effects felt by valence electrons of different angular momentum; this price was by far outweighed by the new ability of pseudopotentials: to predict equilibrium geometries, structural energies [8], and more recently extremely accurate phonon spectra [9] of valence-only solids and molecules with a relatively small plane-wave basis set. In 1985 they thus provided a natural environment for the implementation of the powerful Car-Parrinello theory, by which the simultaneous time evolution of both ions and electronic wavefunctions became possible [1].

Electron-ion pseudopotentials turned out to be a necessary ingredient also for (more recent) stochastic approaches to the exact many-electron hamiltonian and ground-state wavefunction, like variational or diffusion Monte Carlo: even for QMC, up to now, the complication of a nonlocal valence-only ion has been by far preferable over the multiplicity of length and energy scales intrinsic to full-core atoms [10].

1.3 *Who cares about cores?*

Approximate pseudoatoms are much simpler than true atoms, and even so pseudopotential simulations of large-scale molecular or solid-state systems remain a formidable computational task. Standard first-principles pseudopotentials need as many as 200 plane waves per atom for a really accurate description of simple s - p systems (i.e., a 20 Ryd energy cutoff in the case of, say, silicon), and thus many more for “tough” (but unfortunately very interesting) elements like carbon, oxygen, or first-row transition metals. Even if softer pseudopotentials (e.g. of the Vanderbilt type [11]) are adopted, Car-Parrinello simulations of hundreds of pseudoatoms require huge amounts of computer memory and time, and are seldom fully converged. For a given system size, full-core approaches within the DFT (like LMTO or LAPW [4, 6]) end up with a computational effort which is not too different from a pseudopotential calculation, but, as mentioned, they cannot presently compete with plane waves as far as moving ions are concerned [7]. To find an alternative to pseudopotentials and describe,

within the DFT, the molecular dynamics of full-core systems at a similar cost as pseudo systems (thus getting rid of pseudopotential approximations), represents a remarkable goal.

More good reasons to seek new ways of describing full-core systems can be found outside the context of DFT. Key aspects of the electron correlation in many interesting materials are not adequately described by approximate density functionals, and QMC methods are becoming a viable tool to study electron correlations exactly. For this new family of stochastic many-body approaches isolated atoms (unlike LDA, where, using a radial logarithmic grid, they are a matter of seconds on any PC) turn out to be as difficult as polyatomic systems for $Z > 10$ [12]. A consistent construction of pseudopotentials from isolated atoms is therefore impossible (except for very light atoms [13]), and ionic pseudopotentials are thus normally obtained from LDA atoms and later used for QMC simulations [10]. This strategy is tenable for simple s - p systems [14], but not for transition metals and other very interesting elements; its main justification is really the lack of any viable alternative.

In conclusion, new methods aimed at full-core systems are both a desirable complement to existing DFT schemes and a necessary step forward in modern QMC methods.

2 Method

2.1 Background

Recently, in the context of DFT and pseudopotentials, F. Gygi [15] has shown that non-linear coordinate transformations can provide a very efficient tool to reduce the size of the plane-wave set needed to describe a polyatomic system without reducing the accuracy of the calculation, or, in other words, that a given number of plane waves (equivalently, of spatial grid points) can describe a polyatomic system more accurately with CC than with regular euclidean coordinates.¹ The new coordinates must become “denser” where the wavefunctions vary more rapidly (e.g. near atoms and in the bond region for a covalent system), and less dense elsewhere (the interstitial regions). This can be efficiently accomplished by energy minimization (adaptive coordinates), as originally proposed by Gygi, but also, as he later showed [17], by hanging to each atom of the molecule or solid under consideration an appropriate spherical deformation of the euclidean coordinates.

Gygi’s CC have been successfully applied by other groups; the applications have concerned pseudopotentials, valence-only systems and density functionals [18, 19]. In this work we extend Gygi’s CC to full-core systems. Such a possibility was mentioned some time ago [20] and a very recent attempt in this direction has just been published [21], but, as we will try to explain shortly, it bears little resemblance to ours. Besides the advantages of CC for DFT studies of full-core systems, we propose here QMC simulations of full-core electronic systems as a new possible field of application; this idea was stimulated by a recent remarkable contribution of C. Umrigar, not based on CC [22].

2.2 Basic idea

Three elements are at the origin of our work: Gygi’s new method, a reconsideration of full-core approaches based on augmentation, and the idea that CC may become a general tool to study true atoms (made of core and valence electrons) even outside context of DFT, for example within QMC methods.

The partition of space in terms of atomic spheres and interstitial regions, typical of e.g. LAPW, can be revisited in terms of Gygi’s new concepts. In the interstitial regions the

¹A similar “local scaling” transformation was independently proposed for isolated atoms by Ludeña and coworkers with the rather different scope of constructing orbital-free energy-density functionals [16].

electronic wavefunctions are quite smooth, and the uniform, low spatial resolution provided by a few plane waves is adequate. In the atomic spheres, where core and valence wavefunctions undergo rapid spatial variations, the plane waves are augmented by atomic functions given on a radial logarithmic grid; such a high spatial resolution is equivalent to a strong spherical deformation of the euclidean space around each nucleus. However in these methods the different spatial resolution adopted for different regions of space is not defined through a single, continuous, non-euclidean metric tensor; it instead undergoes a sharp discontinuity at the boundaries, which makes these methods radically different (and more involved) than those based on a fixed basis set, like ordinary plane waves.

In this work we propose (and numerically test for isolated atoms) the idea that a suitable, continuous, non-euclidean metric tensor, can account for the strong inhomogeneities of a real electronic system, or, in other words, that $-Z/r$ nuclear potentials, core electrons, and valence electrons, can all be efficiently represented on a suitable set of spatially continuous, energy-independent basis functions of the Gygi type. Besides DFT applications, we will try to show that such a CC transformation may be a promising tool for QMC methods.

2.3 The radial transformation

The key ingredient of our method is a coordinate transformation which deforms the euclidean space around each atom in such a way as to mimic a logarithmic grid in the core region and to smoothly merge into a uniform grid away from it. Our transformation has the same goal as that independently proposed by Modine *et al.* [21], but it's based on a quite different strategy, and, in our intentions, it should be much simpler and more physically transparent. Their rather complicated two-step procedure breaks many symmetries and is neither a true adaptation, nor a coordinate transformation which explicitly follows the ionic positions. Ours preserves all crystal symmetries, being based on the superposition of spherical deformations centered on the atoms. Around each atom we propose a strong radial deformation $\nu(\rho)$, whose range ρ_o approximately corresponds to the covalent radius:

$$r = f(\rho) = C\rho \exp(b\rho) \exp\left[-\left(\frac{\rho}{\rho_o}\right)^4\right] + \rho \left\{1 - \exp\left[-\left(\frac{\rho}{\rho_o}\right)^4\right]\right\} = [1 + \nu(\rho)]\rho \quad (1)$$

Here ρ is the new radial coordinate, r the actual distance from the nucleus, and ν the radial deformation with respect to the euclidean case $r = \rho$. The above transformation, optimized for the isolated silicon atom, is shown in the upper left panel of Fig. 1 ; its purpose is to shift spatial resolution from the valence to the core region, so that core and valence shells acquire a similar length scale in the new radial coordinate (see Fig. 2).

The transformation (Eq. 1) was chosen to satisfy the following properties:

- (a) unlike the logarithmic mesh, it maps $(0, \infty)$ into $(0, \infty)$, to allow the superposition of many such transformations centered at different sites, and thus a generalization to polyatomic systems;
- (b) in the origin it recovers a regular, linear behavior $r = C\rho$;
- (c) it goes back to “flat-space” $r = \rho$ outside the atom;
- (d) it's logarithmic-like in between;
- (e) it's invertible and differentiable.

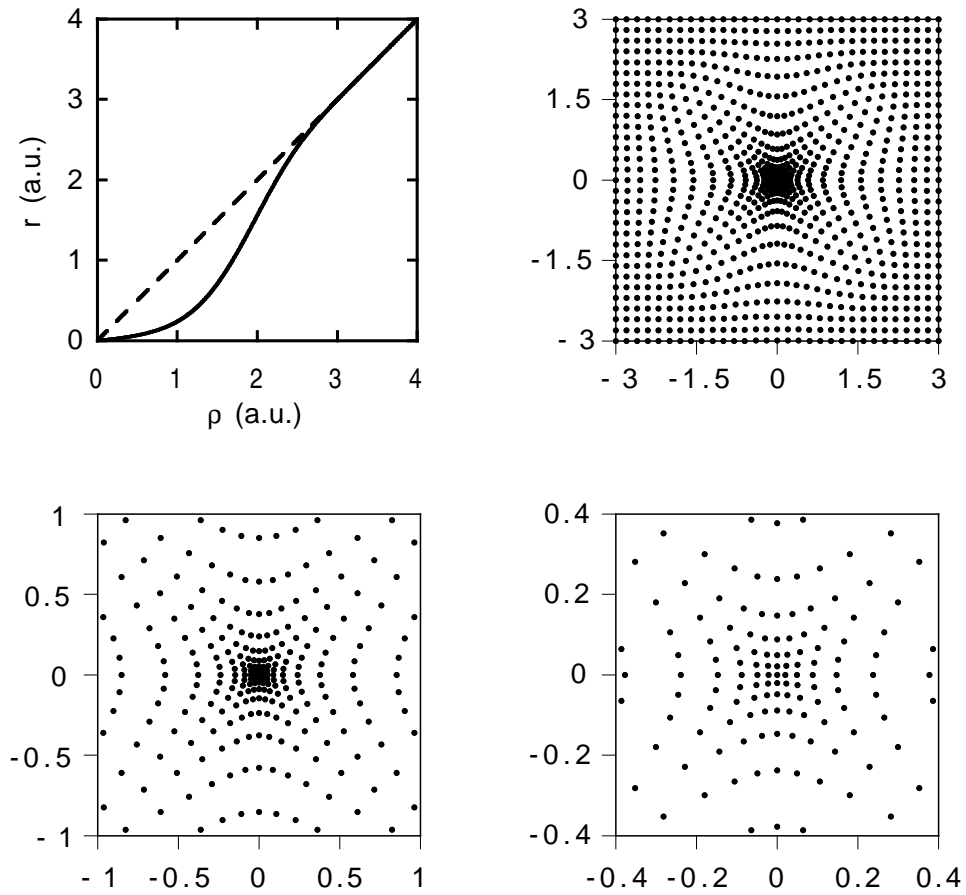


Figure 1: Coordinate transformation for atomic silicon. Upper left panel: radial transformation $r = f(\rho)$ (Eq. 1, solid curve); $r = \rho$ is shown as a dashed line. Upper right panel and lower panels: a 2D uniform grid $\vec{\rho}$ maps into a real-space 2D nonuniform grid \vec{r} (dots). We need three different length scales to appreciate the effect of our transformation (see text).

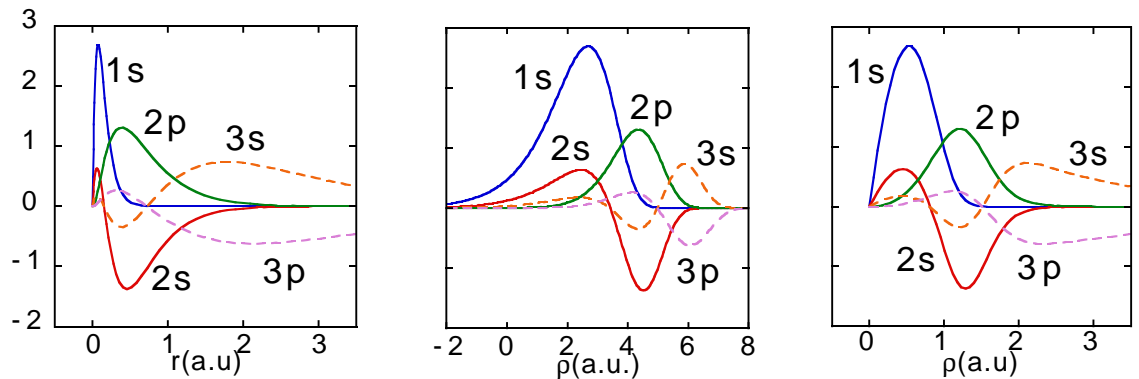


Figure 2: Radial wavefunctions $u_{nl} = rR_{nl}$ for atomic silicon as a function of the distance from the nucleus. Left: ordinary radial coordinate r . Center: logarithmic radial coordinate $\rho = \ln(r/r_0)/\alpha$ with $\alpha = 1$ a.u. Right: radial coordinate $\rho = f^{-1}(r)$ (the inverse of our Eq. 1, Fig. 1). As a function of r (left) the core and valence wavefunctions have a very different length scale, but on a logarithmic grid (center) or using our radial transformation (right) they acquire a similar length scale.

In a molecule or a crystal the spatial CC transformation is obtained as a superposition of spherical deformations $\nu(\rho)$ centered on the atoms:²

$$\vec{r} = \vec{\rho} + \sum_{\alpha} (\vec{\rho} - \vec{R}_{\alpha}) \nu_{\alpha}(|\vec{\rho} - \vec{R}_{\alpha}|) \quad (2)$$

In the upper right panel and in the two lower panels of Fig. 1 we show how a uniformly spaced two-dimensional grid in the new coordinates $\vec{\rho} = (\xi, \eta)$ maps into a nonuniform grid of real-space points $\vec{r} = (x, y)$ (shown as dots) for an isolated silicon atom, placed in the origin. In the upper right panel $(x, y) \in (-3, 3)$ a.u. Near the borders of the square, for $r > 2$, our transformation recovers the identity $\vec{r} = \vec{\rho}$, and a uniform $\vec{\rho}$ grid maps into a uniform $\vec{r} = \vec{\rho}$ grid. Towards the atom the \vec{r} grid points become denser, and cannot be resolved by eye.

We then try to zoom in, but even in the lower right panel, $(x, y) \in (-1, 1)$ a.u., we cannot resolve the \vec{r} grid points of the inner region: between $r = 0.2$ and $r = 2$ the transformation mimics a logarithmic grid, and the more we approach the nucleus, the higher is the density of \vec{r} points. By further zooming in, for $(x, y) \in (-0.4, 0.4)$ a.u. (lower right panel), our eye finally appreciates, below the $1s$ radius (compare to Fig. 2), the recovery of a uniform grid, as implied by the properties (a) and (b) of Eq. 1: very close to the nucleus our transformation recovers a linear behavior $\vec{r} = C\rho$ (with $0 < C \ll 1$).

Fig. 2 shows that the effect of our transformation (right panel) is, as desired, similar to that of a logarithmic grid (center panel); the two main differences are related to the properties (a-c), i.e., the behavior near the origin and the recovery of a uniform euclidean resolution beyond the outermost peak of the valence shells. Figs. 1 and 2 refer, as said, to the silicon atom. Of the three parameters which characterize the transformation Eq. 1 one, ρ_o , it's approximately equal to the covalent radius because of the property (c), and thus practically fixed; the other two, C and b , are positive parameters which are optimized for each particular atom to “equalize” core and valence resolution. Their values, for silicon as well as the other atoms considered in this work, are given in Table 1.

To equalize core and valence resolution amounts to increasing the spatial resolution in the core region and to decreasing it in the outer valence region in such a way as to recover a uniform resolution outside the atom. The effect is illustrated for the silicon atom in Fig. 3, where two key differential properties of our radial transformation are shown. In the left panel we subtract the unity from the radial resolution corresponding to our transformation (Eq. 1 and Fig. 1). In this way we visualize the comparison between our new radial resolution $d\rho/dr$ and the uniform, unit radial resolution of the identical transformation $\rho = r$ (i.e., of ordinary euclidean coordinates). Where $d\rho/dr - 1$ is positive we are gaining radial resolution; where it's negative we are losing radial resolution; where it's zero (outside the covalent radius) we recover the unit resolution of ordinary euclidean coordinates.

The same comparison is shown in the right panel, but now for the *volume* resolution. Here (solid line) we subtract the unity from our volume resolution $\rho^2 d\rho/r^2 dr$.

Again, where $(\rho^2 d\rho/r^2 dr) - 1$ is positive, in the inner atomic region, we are gaining volume resolution; where it's negative, in the outer valence region, we are losing volume resolution; where it's zero, outside the covalent radius, we have the same resolution as ordinary euclidean coordinates.

Our new CC are given in terms of the radial transformation Eq. 1, and the radial resolution (left panel) is certainly interesting, but the volume resolution (right panel, solid line), which is the jacobian determinant of the spatial transformation ([15, 17]), is in fact the right

²Since we give the radial transformation as $r(\rho)$ and not as $\rho(r)$, Eq. 2 is more convenient than Gygi's definition [17]; they become identical only if the deformations relative to different atoms do not overlap.

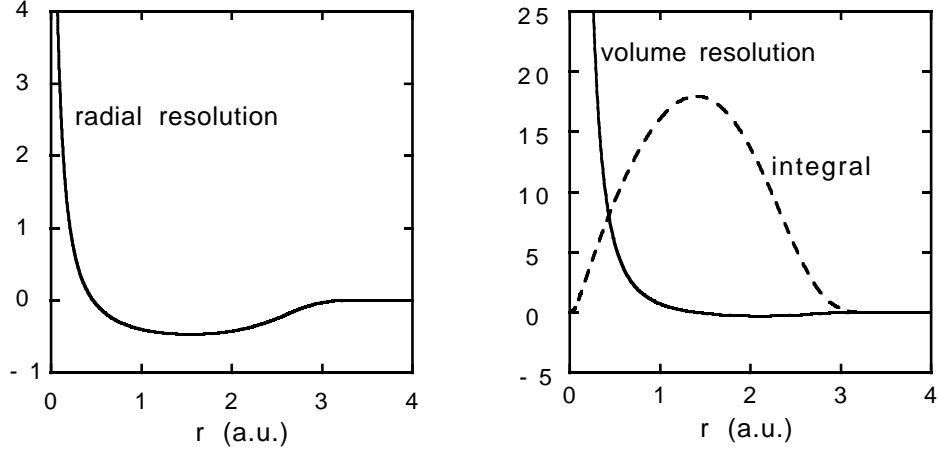


Figure 3: Left: $(d\rho/dr) - 1$, difference between the radial resolution $(d\rho/dr)$ of the new CC (Eq. 1 and Fig. 1) and 1, the uniform radial resolution of ordinary euclidean coordinates. Right, solid line: $(\rho^2 d\rho/r^2 dr) - 1$, difference between the volume resolution of the new CC and the uniform volume resolution of ordinary euclidean coordinates. Right, dashed line: volume integral of $(\rho^2 d\rho/r^2 dr) - 1$ (see text).

thing to look at when comparing the local resolution of the new coordinate system against euclidean coordinates. Let us thus concentrate on the right panel of Fig. 3. Below $r = 1.5$ a.u. there is a large gain in the volume resolution (a larger and larger gain as the nucleus is approached: here the highest resolution is needed, because both core and valence wavefunctions oscillate rapidly); this gain is compensated by a slight loss above $r = 1.5$ a.u., where the valence wavefunctions have their outermost maximum.

The compensation of a gain with a loss is inevitable when the deformation of the euclidean coordinates is confined within a finite volume V and vanishes outside it: in our case the atomic volume, approximately defined by the covalent radius due the property (c). Such a compensation corresponds in fact to a simple conservation law, illustrated by the dashed curve in the right panel. The dashed curve represents the volume integral of the volume resolution, and falls to nothing outside the atom, telling that a finite volume of the $\vec{\rho}$ space (in our case a sphere of radius r_{cov}) maps into the same finite volume of the \vec{r} space (a sphere of radius $\rho_{cov} = r_{cov}$).

The condition (c) could in principle be relaxed to allow $r = \gamma\rho$ with $\gamma > 0$ but different from unity outside the atomic volume V ; in this case the ordinary atomic volume $V = \frac{4}{3}\pi r_{cov}^3$ maps into a different CC atomic volume $V' = \frac{4}{3}\pi \rho_{cov}^3 = V/\gamma^3$, and, in a crystal, lattice constants and reciprocal vectors for euclidean coordinates and CC would differ by a scale factor γ . For $\gamma > 1$ this would amount to a net saving of some useless volume resolution in the interstitial regions, which at first sight could seem an advantage. However, until the CC transformation is just a sum of spherical deformations centered in the atoms as in Eq. 2, such a choice would reduce the volume resolution not only in the empty interstitial regions, but also in the midbond region, which is a great disadvantage; that's why we kept the property (c) as it is. In fact (as illustrated by Fig.4 which shows the CC appropriate to a silicon dimer), even with $\gamma = 1$, our superposition of atomic deformations suffers of some loss of resolution in the bond region. This is inevitable, because we have optimized our transformation in the isolated atom, where we gain resolution in the core region at the expense of the valence region; for this reason, as we will see in the next section, full-core atoms will require an effort which is affordable and much smaller than with euclidean coordinates, but still larger than pseudo atoms.

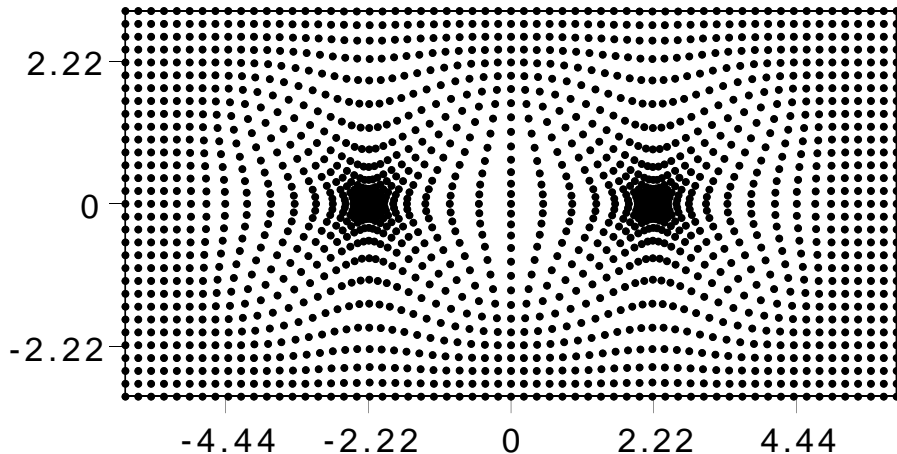


Figure 4: Coordinate transformation for a silicon dimer. A 2D uniform grid $\vec{\rho}$ with $\Delta\rho_x = \Delta\rho_y = 0.2$ a.u. maps into a real-space 2D nonuniform grid \vec{r} (dots). Blowing up the inner-core region (black spots) yields identical results as the isolated atom (Fig. 1).

From Fig. 4 we see that, to further improve the efficiency of our superposition of atomic deformations in a molecule or a solid, it would be good to shift some useless volume resolution away from the empty regions and bring it into the bond region. For this aim a better idea than playing with γ would probably be to add to the superposition of atomic deformations Eq. 2 some appropriate deformation centered at the interstitial sites or in the midbond. This kind of upgrade can further improve the efficiency of the atomic results presented here, and must be tested and optimized in the molecule or solid.

Here we limit ourselves to the atomic transformations, and in the following Sec. 3 we will test them in two ways: generalized plane waves within LDA (3.1), and variational Monte Carlo (3.2).

3 Atomic results

3.1 LDA: generalized plane waves

With our new CC the core and valence radial wavefunctions acquire a similar length scale (Fig. 2); as a consequence, their representation in terms of the corresponding Gygi’s generalized plane waves [15, 17] converges for a much smaller wavevector q than it would happen with regular plane waves and euclidean coordinates. This is clearly illustrated by Fig. 5. In the left panel we plot, as a function of the wavevector q , the ordinary Fourier transforms of the 1s, 2s, and 3s wavefunctions of the isolated silicon atom (obtained from a self-consistent LDA calculation). In the right panel we plot the corresponding “Gygi transforms” on the same scale.³

While the absolute value of the ordinary Fourier transforms (left) drops below a tenth of the full scale of Fig. 5 only for $q > 25$ a.u. (corresponding to a plane-wave cutoff energy $E_{cut} \gg 625$ Ryd) and remains well above one hundredth of the full scale of Fig. 5 even at $q = 40$ a.u. ($E_{cut} = 1600$ Ryd), the absolute value of the corresponding Gygi transforms drops below a tenth of the full scale of Fig. 5 already by $q = 9$ a.u. ($E_{cut} = 81$ Ryd), and below one hundredth between $q = 11$ and $q = 12$ a.u. ($E_{cut} = 144$ Ryd); it becomes

³We only show $q \geq 5$ to emphasize the high- q convergence. For $q < 5$ (not shown) the absolute value of Fourier and Gygi transforms is similar, and much larger: for the n, ℓ shown in Fig. 5 they range from twice to ~ 120 times its full scale.

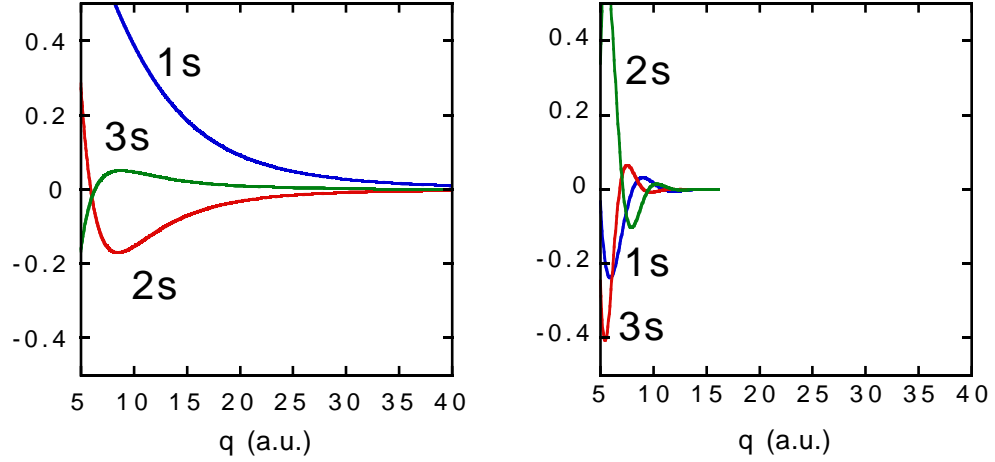


Figure 5: Fourier transform (left) and Gygi transform (right) for the radial s wavefunctions of an isolated atomic silicon.

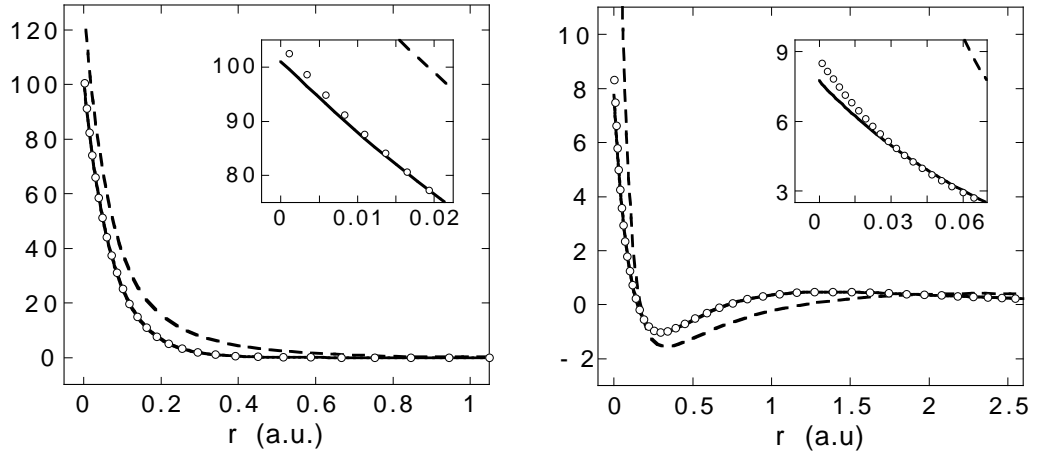


Figure 6: Comparison of the fully converged $1s$ (left) and $3s$ (right) radial wavefunctions of silicon, shown as solid lines, and the backtransformation of their Gygi transforms with $E_{cut} = 25$ Ryd (dashes) and $E_{cut} = 100$ Ryd (empty dots). By $E_{cut} = 100$ Ryd the functions are perfect everywhere except very close to the origin (see insets and text).

completely invisible, on the scale of our plot, for $q > 14$ a.u. ($E_{cut} \simeq 200$ Ryd).

If we backtransform the right-hand curves of Fig. 5 up to a finite wavevector q_{max} we thus expect a very good convergence for any $q_{max} \geq 9$ ($E_{cut} \geq 81$ Ryd). This is shown in Fig. 6, where we compare the $1s$ (left panel) and $3s$ (right panel) original radial wavefunctions (solid line) with the backtransformation of their Gygi transforms with a low cutoff $q_{max} = 5$ a.u. (dashes) and a high cutoff $q_{max} = 10$ a.u. (empty dots). We have chosen to show the core $1s$ because, as we will see in a moment, it's of crucial importance for the energy convergence, and the $3s$ as a typical valence radial wavefunction, but the same behavior as a function of q_{max} is found for the occupied states of any other n and ℓ . As expected from Fig. 5, by $q_{max} = 10$ a.u. ($E_{cut} = 100$ Ryd) the convergence is so good that we cannot distinguish the original radial wavefunctions from their backtransformed counterparts.

Besides the visual impact of Figs. 5 and 6, it's a good idea to quantitatively check the convergence of the total electronic energy as a function of the cutoff q_{max} , or, equivalently, of the cutoff energy E_{cut} . We do that by cutting off the Gygi transforms of all the occupied atomic wavefunctions (shown in Fig. 5 for $\ell = 0$) beyond different q_{max} values, backtrans-

Table 1: Parameters of the transformation (Eq. 1)

	C	b	ρ_0
Li	0.42-0.91	0.1-0.2	1-7
C	0.139	0.75	1.75
Si	0.089	0.75	2.0
U	0.03	0.75	2.3

forming them to real space, and monitoring the resulting total electronic energy as a function of q_{max} .⁴

The results are shown in Table 2 for atomic carbon and silicon; for atomic silicon they are also displayed in the left panel of Fig. 7. The error, shown as a function of the cutoff energy (in Rydbergs), is everywhere defined as the energy deviation (in electron volts) from a perfectly converged real-space LDA atom.⁵

Let us first concentrate on the second column of Table 2, which contains the total-energy error (in electron volts) for the neutral carbon and silicon atoms. We immediately see that, even for the highest cutoffs, the error on absolute total energies is of the order of a few electron volts. This error is in fact of the same order of magnitude as that found by Modine *et al.* on absolute total energies for isolated carbon and oxygen atoms, and could sound as a discouraging result: it tells us that a cutoff energy of 100 – 150 Ryd, which corresponds to visually perfect backtransforms of the atomic wavefunctions (Fig. 6), yields an error which is certainly tiny on the scale of the core and total atomic energies (one to two parts per thousand), but unfortunately still sizable on the scale of the physically relevant valence energies. We have tried to carefully analyze the origin of such an absolute total-energy error, since we suspected, on transparent physical grounds, that it cancels out in binding energies and other differential valence properties. Our finding is that the error mostly comes from the $1s$ state, and is indeed almost independent of the valence configuration. A simple mathematical argument shows that our transformation can greatly reduce, but not eliminate, the problem of the electron-nuclear cusp.⁶ Such an origin of the eV -sized error in the total energies is confirmed by monitoring the individual contributions to the total energy, with special attention to $\langle n\ell | -\frac{1}{2}\nabla^2 - Z/r | n\ell \rangle$ [23]. As a result, valence properties can be obtained to a high accuracy with a large but affordable cutoff: for example a ~ 120 Ryd cutoff allows estimates of valence ionization potentials and hybridization energies which are accurate within a few hundredths of an eV for Carbon and Silicon atoms (see Table 2 and Fig. 7). Another way of saying that any total-energy contribution other than $\langle n\ell | -\frac{1}{2}\nabla^2 - Z/r | n\ell \rangle$ converges much faster than it, is to say that our CC are particularly effective for the solution of the electrostatic problem.

For example, by $E_{cut} \simeq 70$ Ryd for the silicon atom, and by $E_{cut} \simeq 170$ Ryd for a huge atom like uranium, the absolute electrostatic energies are within their converged value by less than $0.1eV$; the uranium results compare thus very well with Goedecker’s recent electrostatic investigations based on wavelets [24].

⁴We do not perform a different self-consistent calculation for each q_{max} , but simply expand the self-consistent wavefunctions of a converged real-space atomic calculation in terms of a finite number of Gygi spherical waves [15, 17].

⁵Relativistic and spin-polarization effects are consistently not included in this work, so our results cannot be directly compared to experimental atomic energies.

⁶The cusp also affects the higher s states, but in this case, for obvious reasons, its quantitative impact on total energies is practically negligible.

Table 2: Energy errors* (in eV) versus cutoff energy E_{cut} (in Rydbergs).

	E_{cut}	Total	1st IP	2nd IP	3rd IP	sp ³
carbon	81	8.1634	0.4299	0.7626	-0.9114	-0.8881
	100	8.1090	0.0771	0.1671	-0.0743	-0.2022
	121	3.4015	-0.0016	0.0039	0.0067	-0.0091
	144	1.5238	0.0044	0.0028	-0.0498	-0.0251
silicon	100	22.340	0.172	0.154	-0.562	-0.587
	121	28.436	0.038	-0.045	0.033	0.011
	144	15.701	0.030	-0.045	0.073	0.043
	169	5.932	0.033	-0.040	0.019	0.004

*Total: total energy; IP: ionization potential; sp³: hybridization energy. Beyond $E_{cut} \simeq 100$ Ryd the error on valence energies (last four columns), which are total-energy differences, is very small.

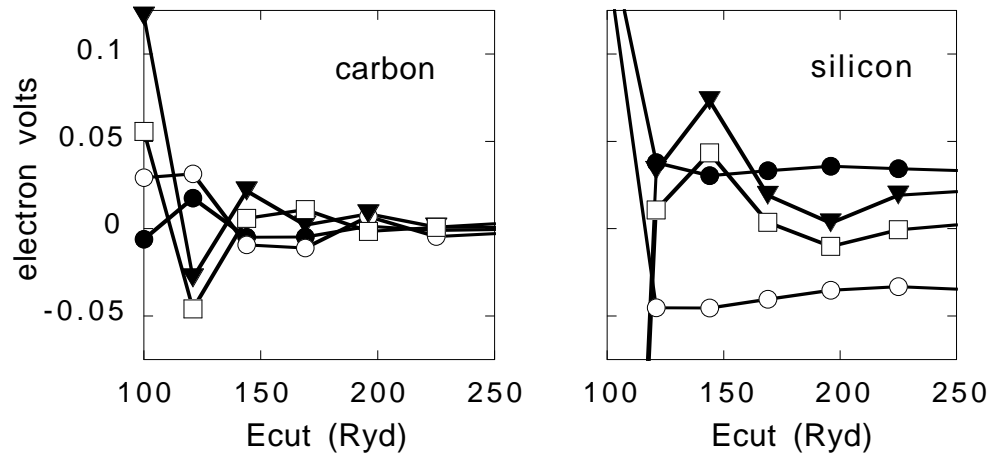


Figure 7: Error on the ionization potentials (1st: full dots; 2nd: empty dots; 3rd: full triangles) and on the hybridization energy (empty squares) as a function of the cutoff. Beyond $E_{cut} \simeq 120$ Ryd the errors on these valence energy differences are hundredths of an eV , although the two individual atomic energies still suffer from an error in the eV range. Left: carbon. Right: silicon.

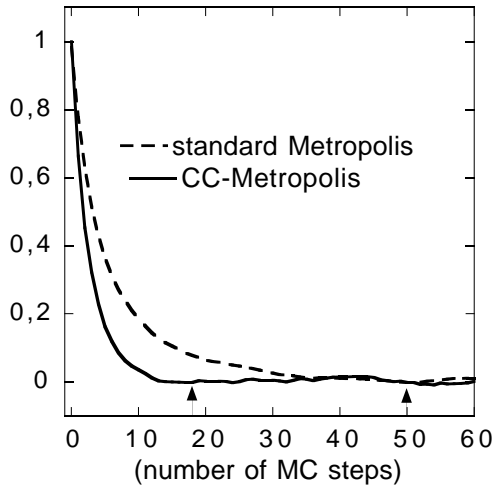


Figure 8: Energy autocorrelation function for the standard Metropolis algorithm (dashed line) and for the CC Metropolis algorithm (solid line), when used for the lithium atom. The two arrows approximately indicate the autocorrelation time in either case.

It's of course very easy to test our CC for self-consistent Kohn-Sham atoms in real space, by simply generalizing the usual algorithm for logarithmic grids [5] to any radial grid. Accurate ionization potentials and hybridization energies are obtained with much less grid points than total energies, but even absolute total energies converge quickly with the number of grid points (more quickly than they do with the maximum wavevector in the previous examples), because here the usual Taylor expansion near the origin takes care of the electron-nuclear cusp problem [23]. This finding serves thus only as a final confirmation of our analysis of the total-energy error found with generalized plane waves: for truly three-dimensional real-space calculations (solids or supercell molecules) based on CC we don't have at hand an easy way to take advantage of the exact Taylor expansion near the nucleus, and thus we expect a similar performance as the generalized-plane-wave expansion of the previous subsection 3.1: good valence energies in spite of fair total energies.

Although accurate valence properties represent already a remarkable achievement, it would be of course very desirable to have an efficient way of totally defeating the electron-nuclear cusp both in generalized plane waves and in three-dimensional real space. An easy remedy, suggested by Modine *et al.*, is to replace the nuclear point charge with a gaussian charge whose range is much smaller than the $1s$ radius. Unfortunately, by doing that, the resulting absolute total-energy error is still in the eV range for atoms like carbon or silicon (i.e., of the same order of magnitude as doing nothing), as can be easily understood and numerically checked; however, in the lack of better ideas, such a remedy can become of interest when moving ions in a Car-Parrinello molecular-dynamics simulation.

3.2 Variational Monte Carlo

In this section we show preliminary results for the isolated lithium atom which suggest that a straight Metropolis sampling in the new CC improves the sampling efficiency by a factor of three with respect to a straight Metropolis sampling in the ordinary euclidean coordinates. This new application of CC was somewhat inspired by a recent contribution of C. Umrigar in the field of Variation Monte Carlo methods [22]. He has proposed a generalized Metropolis scheme which, by a smart modification of the proposal matrix, obtains tiny correlation times

and high acceptance rates, thus efficiently reducing the inconvenience of multiple length scales of electrons in real isolated atoms. His (rather impressive) results concern both first-row elements, and the heavier argon atom ($Z = 18$), but, unlike CC, cannot be easily generalized to polyatomic systems. When plugged into the variational Monte Carlo scheme, a CC transformation modifies the proposal matrix with respect to a standard Metropolis sampling and can be tailored to correspondingly reduce the autocorrelation time in a similar, but simpler way, as the Accelerated Metropolis algorithm of Umrigar [22]. With respect to his approach our coordinate transformation shares a variable length for the proposed step as a function of the distance from the nucleus. In the preliminary results presented here we don't take any further advantage of the wavefunction (as Umrigar, instead, does [22]); so our minimum autocorrelation time will still correspond to an acceptance ratio of $\sim 50\%$, and we expect an interesting, but less pronounced improvement over straight Metropolis MC, than him. In Fig 8 we show the energy autocorrelation function obtained from standard and CC Variational Monte Carlo runs for the lithium atom [23]. We do find a reduced correlation time (by a factor of ~ 3). Similar results can be obtained with a relatively wide range of parameters (see Table 1; the results of Fig 8 correspond to the particular choice $C = 0.42$, $b = 0.2$, $\rho_o = 7$). As expected, this is good but less spectacular than Umrigar's results. The real advantage of our approach based on CC is that it lends itself to a simple and natural generalization to polyatomic systems. Our VMC experiment in CC is the first step in an entirely new direction; many more are of course needed to explore (and possibly establish) the general convenience of CC within QMC methods. We are presently experiencing on atoms with more shells than lithium and trying to incorporate the remainder of Umrigar's method into our scheme.

4 Conclusions and perspectives

The atomic shell structure originates from the peculiar radial dependence of the electron-nuclear potential $-Z/r$ and from the Fermi statistics; its typical multiplicity of length scales is not dramatically altered by the electron-electron repulsion, and is thus intimately related to the electron-nuclear distance. Starting from F. Gygi's ideas, we have proposed a CC transformation which can stretch electron-nuclear distances, works for valence properties of full-core LDA atoms, and seems to improve variational Monte Carlo simulations of full-core atoms. The atomic results of this paper represent an encouraging starting point for further developments and applications, which are underway: on one hand, plane-wave and real-space LDA calculations of full-core crystals and molecules; on the other, more investigations in the field of quantum Monte Carlo.

Acknowledgements

We are grateful to C. Filippi for her precious training and assistance in the initial part of our VMC work, and to F. Gygi, G. Galli, S. Moroni and C. Umrigar for very useful conversations. GBB gratefully acknowledges partial financial support from the Italian National Research Council (CNR, Comitato per la Scienza e la Tecnologia dell'Informazione, grants no. 96.02045.CT12 and 97.05081.CT12).

References

- [1] R. Car and M. Parrinello, Phys. Rev. Lett. **55**, 2471 (1985).

- [2] see e.g. D.M. Ceperley and L. Mitáš, *Advances in Chemical Physics, Volume XCIII*, edited by I. Prigogine and S.A. Rice (Wiley 1996); J.C. Grossman and L. Mitáš, *Phys. Rev. Lett.* **22**, 4353 (1997), and references therein.
- [3] D.R. Hamann, M. Schlüter, and C. Chiang, *Phys. Rev. Lett.* **43**, 1494 (1979); G.B. Bachelet, D.R. Hamann, and M. Schlüter, *Phys. Rev.* **26**, 4199 (1982).
- [4] O.K. Andersen, *Phys. Rev. B* **12**, 3060, (1975).
- [5] D. Liberman, J.T. Waber, and D.T. Cromer, *Phys. Rev.* **137**, A27 (1965).
- [6] M. Methfessel, *Phys. Rev. B* **38**, 1537 (1988); M. Methfessel, C.O. Rodriguez, and O.K. Andersen, *ibid.* **40**, 2009 (1989); see also *Full-Potential LMTO for Crystals*, M. Methfessel and M. van Schilfgaarde, this volume.
- [7] see e.g. *Plane waves, Pseudopotentials, and the LAPW Method*, by D.J. Singh, Kluwer Academic Publishers, Boston 1993; also B. Kohler, S. Wilke, M. Scheffler, R. Kouba, and C. Ambrosch-Draxl, *Comput. Phys. Commun.* **94**, 31 (1996).
- [8] M.T. Yin and M.L. Cohen, *Phys. Rev. Lett.* **45**, 1004 (1980); *Phys. Rev. B* **26**, 3259 (1982); *ibid.*, 5668 (1982).
- [9] S. Baroni, P. Giannozzi, and A. Testa, *Phys. Rev. Lett.* **58**, 1861 (1987).
- [10] S. Fahy, X.W. Wang, and S.G. Louie, *Phys. Rev. Lett.* **61**, 1631 (1988); *Phys. Rev. B* **42**, 3503 (1990); G.B. Bachelet, D.M. Ceperley, and M. Chiocchetti, *Phys. Rev. Lett.* **62**, 2088 (1989); X.P. Li, D.M. Ceperley, R.M. Martin e E.L. Shirley, *Phys. Rev. B* **42**, 3503 (1990); A. Malatesta, S. Fahy, and G.B. Bachelet, *Phys. Rev. B* **56**, 12201 (1997).
- [11] D. Vanderbilt, *Phys. Rev. B* **41**, 7892 (1990).
- [12] D.M. Ceperley, *J. Stat. Phys.* **43**, 815 (1986); see also Ref. [22], and references therein.
- [13] P.H. Acioli and D.M. Ceperley *J. Chem. Phys.* **100**, 8169 (1994).
- [14] E.L. Shirley, R.M. Martin, G.B. Bachelet, and D.M. Ceperley, *Phys. Rev. B* **42**, 5057 (1990); P. Focher, A. Lastrì, M. Covi, and G.B. Bachelet, *Phys. Rev. B* **44**, 8486 (1991).
- [15] F. Gygi, *Europhysics Letters* **19**, 617 (1992); F. Gygi, *Phys. Rev. B* **48**, 11692 (1993).
- [16] E.S. Kryachko and E.V. Ludeña, *Phys. Rev. A* **43**, 2179 (1991); see also R. Lopez-Boada, E.V. Ludeña, V. Karasiev, and R. Pino, *J. Chem. Phys.* **107**, 6722 (1997), and references therein.
- [17] F. Gygi, *Phys. Rev. B* **51**, 11190 (1995); F. Gygi and G. Galli, *ibid.* **52**, R2229 (1995).
- [18] D.R. Hamann, *Phys. Rev. B* **54**, 1568 (1996); *ibid.* **56**, 14979 (1997).
- [19] L. De Santis and R. Resta, preprint, <http://xxx.lanl.gov/abs/cond-mat/9712176>.
- [20] A. Devenyi, K. Cho, T.A. Arias, and J.D. Joannopoulos, *Phys. Rev. B* **49**,13373 (1993).
- [21] N.A. Modine, G. Zumbach and E. Kaxiras, *Phys. Rev. B* **55**, 10289 (1997).
- [22] C. Umrigar, *Phys. Rev. Lett.* **71**, 408 (1993).
- [23] A. Putrino, Tesi di Laurea (in Italian).
- [24] S. Goedecker and O.V. Ivanov, preprint, <http://xxx.lanl.gov/abs/physics/9701024>.